

# Performance comparison of shear walls with openings designed using elastic stress and genetic evolutionary structural optimization methods

Hu Z. Zhang<sup>\*1, 2</sup>, Xia Liu<sup>2</sup>, Wei J. Yi<sup>2</sup> and Yao H. Deng<sup>2</sup>

<sup>1</sup>Hunan Provincial Key Laboratory of Structures for Wind Resistance and Vibration Control, Hunan University of Science and Technology, Xiangtan, China

<sup>2</sup>Hunan Provincial Key Lab on Damage Diagnosis for Engineering Structures, Hunan University, Changsha, China

(Received March 29, 2017, Revised November 23, 2017, Accepted December 26, 2017)

**Abstract.** Shear walls are a typical member under a complex stress state and have complicated mechanical properties and failure modes. The separated-elements model Genetic Evolutionary Structural Optimization (GESO), which is a combination of an elastic-plastic stress method and an optimization method, has been introduced in the literature for designing such members. Although the separated-elements model GESO method is well recognized due to its stability, feasibility, and economy, its adequacy has not been experimentally verified. This paper seeks to validate the adequacy of the separated-elements model GESO method against experimental data and demonstrate its feasibility and advantages over the traditional elastic stress method. Two types of reinforced concrete shear wall specimens, which had the location of an opening in the middle bottom and the center region, respectively, were utilized for this study. For each type, two specimens were designed using the separated-elements model GESO method and elastic stress method, respectively. All specimens were subjected to a constant vertical load and an incremental lateral load until failure. Test results indicated that the ultimate bearing capacity, failure modes, and main crack types of the shear walls designed using the two methods were similar, but the ductility indexes including the stiffness degradation, deformability, reinforcement yielding, and crack development of the specimens designed using the separated-elements model GESO method were superior to those using the elastic stress method. Additionally, the shear walls designed using the separated-elements model GESO method, had a reinforcement layout which could closely resist the actual critical stress, and thus a reduced amount of steel bars were required for such shear walls.

**Keywords:** shear wall; openings; genetic evolutionary algorithm; separated-elements model GESO; elastic stress method; structural optimization design

## 1. Introduction

Shear walls, as an important lateral-load-resistant component, are commonly applied to reinforced concrete (RC) structures. Some theoretically validated methods are used for designing them, more often than not, they are designed using empirical design methods based on the assumption that plane section remains plane, which is similar to frame columns. For example, the empirical design methods are provided in code specifications such as the Chapters 11 of the US code (ACI 318-14 2014), Chapter 6 of the Chinese code (GB 50010-2010 2010), and Chapter 7 of the Chinese code (JGJ 3-2010 2010). However, shear walls are a typical two-dimensional member and their behavior may not be fully interpreted based on the plane-section assumption. To satisfy architectural functions, shear walls are designed to have openings, significantly complicating the design of their reinforcement layouts. In order to improve the design accuracy, the Strut-and-Tie Model (STM) method (i.e., elastic stress method) is recommended as an alternative approach to design shear walls to resist horizontal shear forces if they have a height

not exceeding two times the wall length according to the US code (ACI 318-14 2014). Further, the Chinese code (GB 50010-2010 2010) suggests that two-dimensional and three-dimensional members can be designed based on the results from an elastic-plastic stress method in addition to elastic stress method. In other words, the stress method has increasingly gained attention for the design of structural members under a complex stress state.

The evolutionary structural optimization (ESO) method were utilized to optimize the design of a structure through repeating finite element analysis (FEA) and deleting several inefficient elements at each repetition (Querin 1997, Xie and Steven 1993). This method sometimes leads to a local optimal solution as the elements of the structure are deleted unidirectionally. Accordingly, for improvement the Bidirectional ESO (BESO) method (Querin *et al.* 1998, 2000, Yang *et al.* 1999, Young *et al.* 1999, Tang *et al.* 2015), the Smooth ESO (SESO) method (Fernandes *et al.* 2017) and the Genetic ESO (GESO) method (i.e., probabilistic rejected method) (Liu *et al.* 2008) were proposed. The GESO method, initially introduced based on an integrated-elements model, had been used to construct many topology models of D-regions some of which had successfully been applied to deep beams (Liu *et al.* 2010). The combination of the reinforcement and concrete is taken as a composite material in the integrated-elements model

\*Corresponding author, University Lecturer  
E-mail: zhanghz\_hnu@163.com

which allows the concrete involved in the optimization process. It should be noted that due to design considerations only the reinforcement might be expected to be optimized in practical applications, and the separated-elements model GESO method was accordingly proposed to satisfy such needs (Zhang *et al.* 2014, Zhang *et al.* 2017). For the separated-elements model GESO method, reinforcement and concrete elements are built separately but only the reinforcement elements are optimized. The optimization method based on the separated-elements model not only improves the computational accuracy, but yields results closely matching those in the actual situation. And the topology results from such optimization can be directly utilized for the design of RC members, significantly reducing subjective factors during the design process.

Experimental investigation on shear walls has been considerably conducted by researchers in the literature (Christidis and Trezos 2017, Galano and Vignoli 2000, Gulec *et al.* 2008, Javidsharifi 2017, Lao and Han 2011, Liang *et al.* 2011, Pavel and Pricopie 2015, Salonikios and Kappos 1999, Quiroz *et al.* 2013, Tomazevic *et al.* 1996). However, few researches addressed the reinforcement layout optimization for shear walls. The GESO method has been verified against experimental results using deep beams but not shear walls. The purpose of this paper is to verify the adequacy of the separated-elements model GESO method for the design of shear walls through experimental evaluation. Two types of RC shear wall specimens, which had the location of an opening in the middle bottom and the center region, respectively, were utilized for this study. For each type, two specimens were designed using the separated-elements model GESO method and elastic stress method, respectively. The specimens were fabricated, instrumented, and tested in the structural lab. The tests results addressed in this paper encompassed the ultimate bearing capacity (UBC), ultimate displacement, crack and strain developments, failure modes, etc. Through comparison of the behavior of the two specimens of each type designed using different methods, the feasibility and advantages of the separated-elements model GESO method over the traditional elastic stress method were discussed.

## 2. Research significance

The theoretical research on the separated-elements model GESO method was previously introduced and discussed by Zhang *et al.* (2014). However, there is still a lack of comprehensive experimental data for the shear wall specimens designed using this method. This paper provided the experimental verification of the adequacy and feasibility of the separated-elements model GESO method and to highlight its advantages over the traditional elastic stress method. Note the separated-elements model GESO method is essentially an elastic-plastic stress method, so its differences from the elastic stress method were compared accordingly.

## 3. Experimental program

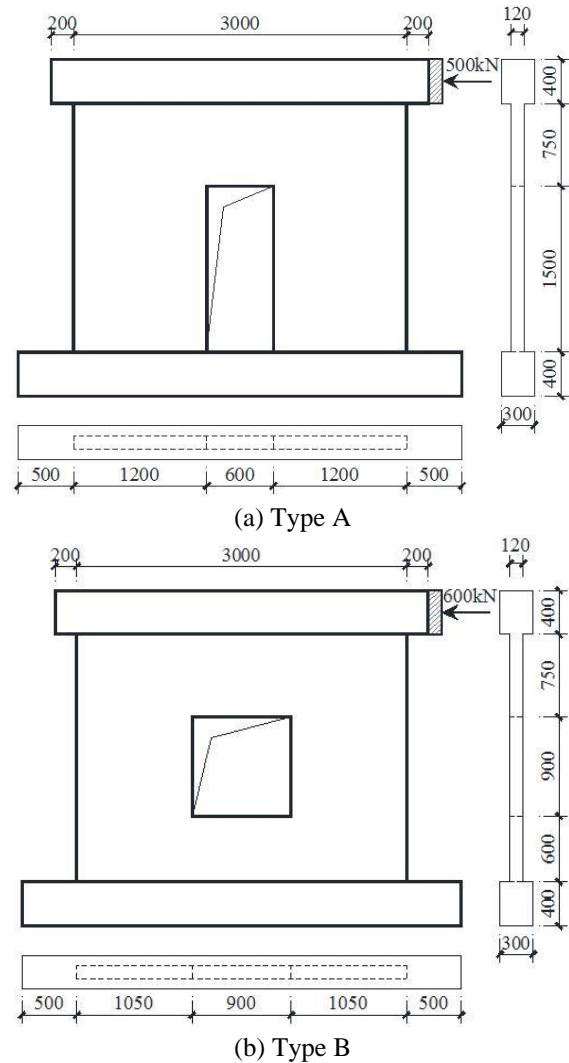


Fig. 1 Dimensions of specimens (Note: dimensions in mm; 1 in. = 25.4 mm; 1 kip = 4.448 kN.)

### 3.1 Specimen details

To make comparison of the separated-elements model GESO and elastic stress methods, four shear wall specimens were designed using the two methods. Each specimen has a length of 3000 mm (118.1 in.), a height of 2250 mm (88.6 in.), and a thickness of 120 mm (4.7 in.). Two types of specimens (two specimens of each type) shown in Fig. 1 encompass: a) Type A-specimens KMQ-1 and KMQ-2, the shear walls with a rectangular opening (600 mm × 1500 mm, 23.6 in. × 59.1 in.) of door in the middle bottom shown in Figure 1(a); and b) Type B-specimens KCQ-1 and KCQ-2, the shear walls with a rectangular opening (900 mm × 900 mm, 35.4 in. × 35.4 in.) in the center region shown in Fig. 1(b). Note that specimens KMQ-1 and KCQ-1 were designed using the elastic stress method, while specimens KMQ-2 and KCQ-2 were designed using the separated-elements model GESO method. The two specimens of each type have identical overall and opening dimensions, design loads, and material properties. Types A and B specimens were subjected to a concentrated horizontal load of 500 kN (112.4 kip) and 600 kN (134.9 kip), respectively. The

horizontal load was applied through a 300 mm (11.8 in.) wide bearing plate to prevent local damage at the specimen upper-right. The design axial compression ratio for all the specimens was 0.1 (i.e., uniform load on the beam top). The bottom surface of the ground beams was restrained and the movement of their left ends was also restricted. The design strength grade of the concrete was Chinese C40, which represents a (150 mm×150 mm×150 mm, 5.9 in.×5.9 in.) characteristic cube concrete compressive strength of 40 MPa (5.8 ksi) with 95% guarantee rate. The steel was Chinese HPB300 with a yield strength of 300 MPa (43.5 ksi), elastic modulus of 210 GPa (30,500 ksi) and Poisson's ratio of 0.3.

Three types of failure modes were found in shear walls (ASCE/SEI 41-06 2007): bending, shearing and bending-shearing failures, which are dependent on the aspect ratios or shear span ratios of shear walls (Salonikios 2002). According to conventional designs, Type A shear walls are classified as a batted wall with an opening area percentage of 13.3% and their limbs have an aspect ratio of 1.875; whereas Type B shear walls are classified as an integral section wall with an opening area percentage of 12.0% and their limbs have an aspect ratio of 0.75. And Type A and Type B shear walls commonly have bending-shearing and shearing failure modes, respectively.

### 3.2 Specimen design using elastic stress method

Specimens KMQ-1 and KCQ-1 were designed using the elastic stress method according to the provision 6.1.2 of Chinese code (GB 50010-2010 2010) (i.e., for the design of two-dimensional and three-dimensional members in non-frame structures, their stress distributions must be derived using an elastic or elastic-plastic analysis method, the quantity of reinforcement can be then determined based on the calculated principal tensile stresses, and their reinforcement layouts can be finalized based on the distribution area of the principal tensile stresses).

The FEA software SAP2000 was used to perform the elastic analysis. The reinforcement layouts for specimens KMQ-1 and KCQ-1 are shown in Fig. 2 with two layers of steel bars in parallel with the facade of the wall body. The two layers of reinforcement located 30 mm (1.2 in.) away from the front and back surfaces of each specimen, respectively, as shown in Fig. 2. Additionally, wire meshes with a steel bar diameter of 5 mm (0.2 in.) and a mesh of 15 mm×15 mm (0.59 in.×0.59 in.) were tied to the outward surface of the entire main reinforcement in order to avoid cracks due to temperature change and concrete shrinkage.

It can be seen from Fig. 2 that there are some unreinforced areas which even fall short of the minimum requirements of the modern codes, for instance, the reinforcements at the upper left corner of the openings are certainly far less than the minimum distributed reinforcements. Due to this fact the cracks might be out of control there. Nevertheless, on one hand, neither tensile stress nor cracks are produced in these areas in the early stage of loading. They are produced till significant stress redistribution occurred there when it is close to failure; on the other hand, the following test focus on the difference in controlling the stress redistribution between elastic stress

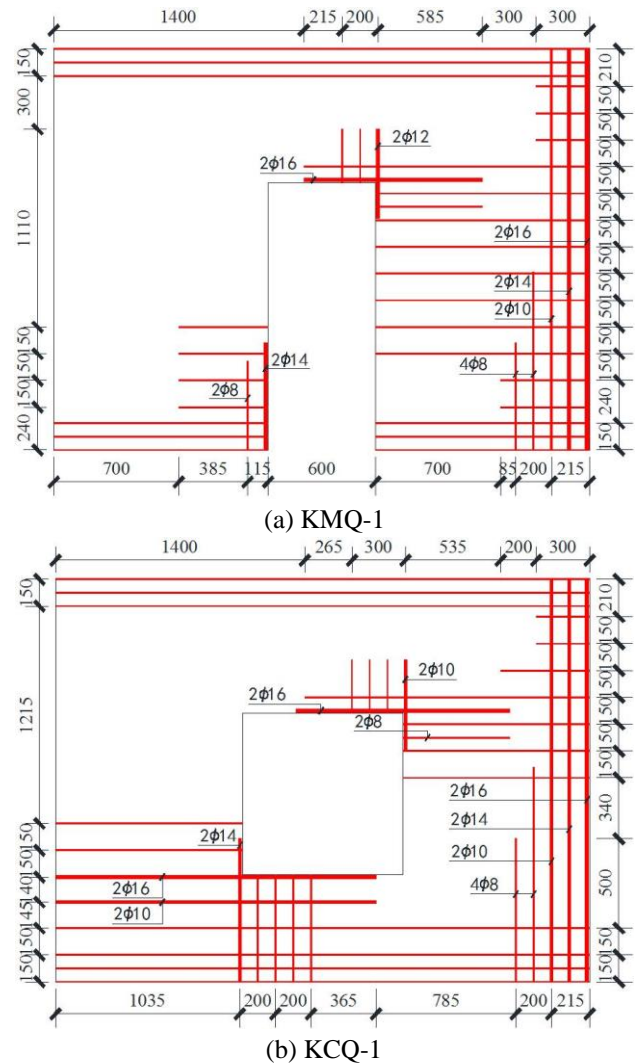


Fig. 2 Reinforcement layout of specimens designed using elastic stress method (Note: dimensions in mm; 1 in. = 25.4 mm;  $\phi 12$  denotes a steel bar, the design  $f_{y,k}$  of which is 300 N/mm<sup>2</sup>, with a diameter of 12 mm; the unspecified ones are steel bars, the design  $f_{y,k}$  of which is 300 N/mm<sup>2</sup>, with a diameter of 6 mm; 1 ksi = 6.895 N/mm<sup>2</sup>)

method and GESO method, while the minimum requirements for reinforcement are mainly the last empirical defense line against collapse. Thus, the reinforcement layouts in this paper are solely based on the FEA results (the reinforcement layouts in the later sections are only based on the optimal solutions on GESO method as well).

### 3.3 GESO

As mentioned previously, the GESO method combines the advantages of the genetic algorithm and ESO method; hence it is easier to find the global optimal solution and has high computational efficiency. In GESO, every element has a chromosome with binary codes and their live genetic codes are '1' at the beginning. Next, some of them become '0' if they are low adaptive value in the copying, crossover, mutation and other 'genetic' processes. The elements with all genetic codes of '0' will be eliminated.

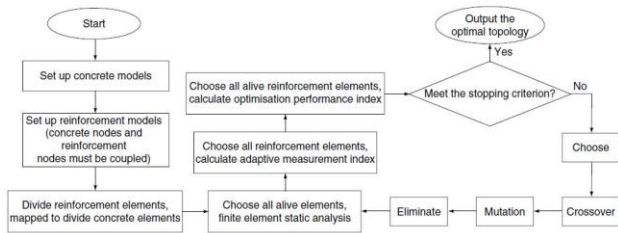
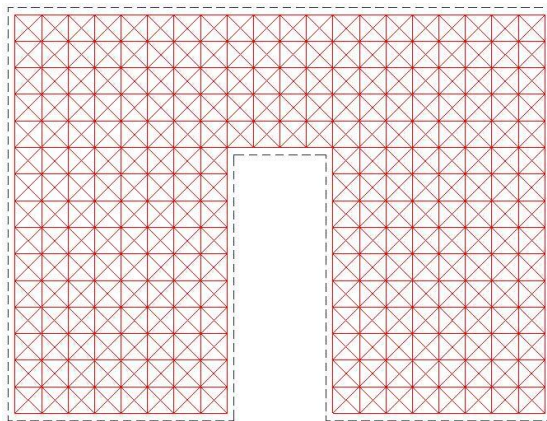
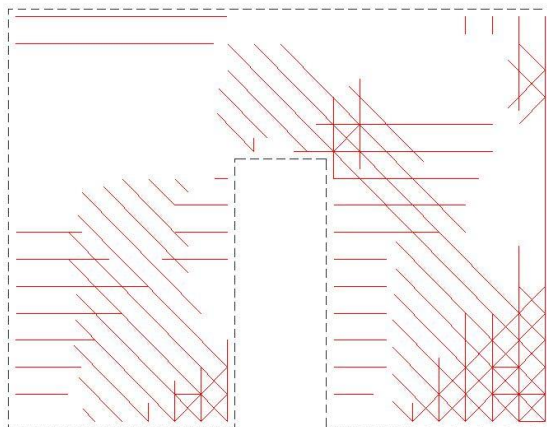


Fig. 3 The flowchart of the separated-elements model GESO method



(a) Initial reinforcement elements

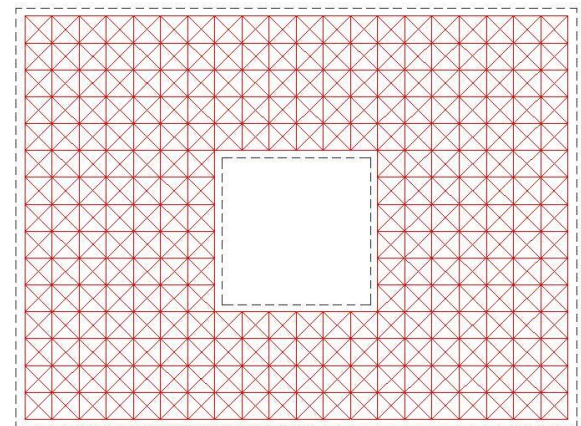


(b) Topological reinforcement elements

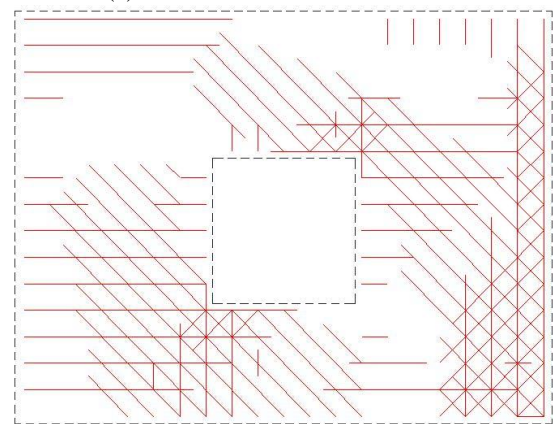
Fig. 4 The process of separated-elements model GESO - specimen KMQ-2

ANSYS FEA software is the main tool, in which the PLANE82 element is usually chosen for simulating RC. After the visual graphics of the topological results are obtained, the investigators may change them into STMs for analysis and design.

FEA of separated-elements model GESO (Zhang *et al.* 2014), chooses different types of elements, which share common nodes, to establish reinforcement and concrete, and concrete cracks are stimulated by a smeared crack model. Once a nonlinear analysis is completed, some inefficient reinforcement elements will be deleted and not participate in the following optimization. The output is calculated and filtered repeatedly, and the process iterates until the optimization results meet the predetermined criteria. Finally, the reinforcement elements are optimized



(a) Initial reinforcement elements



(b) Topological reinforcement elements

Fig. 5 The process of separated-elements model GESO - specimen KCQ-2

and the left are the most efficient reinforcement towards stress. The flowchart of the separated-elements model GESO method is presented in Fig. 3.

### 3.4 Specimen design using separated-elements model GESO method

The separated-elements model GESO method were used to obtain the reinforcement layout of a member under a complex stress state including the location, length, and quantity of steel bars. Again, specimens KMQ-2 and KCQ-2 were designed using this method. Figs. 4(a) and 5(a) show the initial reinforcement elements of specimens KMQ-2 and KCQ-2, respectively. The reinforcement layout has a grid size of 150 mm (5.9 in.) and the diagonal reinforcement with an angle of 45°. Several inefficient reinforcement elements will be deleted in the separated-elements model GESO and the topological reinforcement elements will be obtained as shown in Figs. 4(b) and 5(b) after several generations of selection and elimination. According to these topological results, the reinforcement layouts for specimens KMQ-2 and KCQ-2 were designed as shown in Fig. 6 (note that similar to specimens KMQ-1 and KCQ-1 each specimen has two identical reinforcement layers vertically and two identical wire meshes tied to the two reinforcement

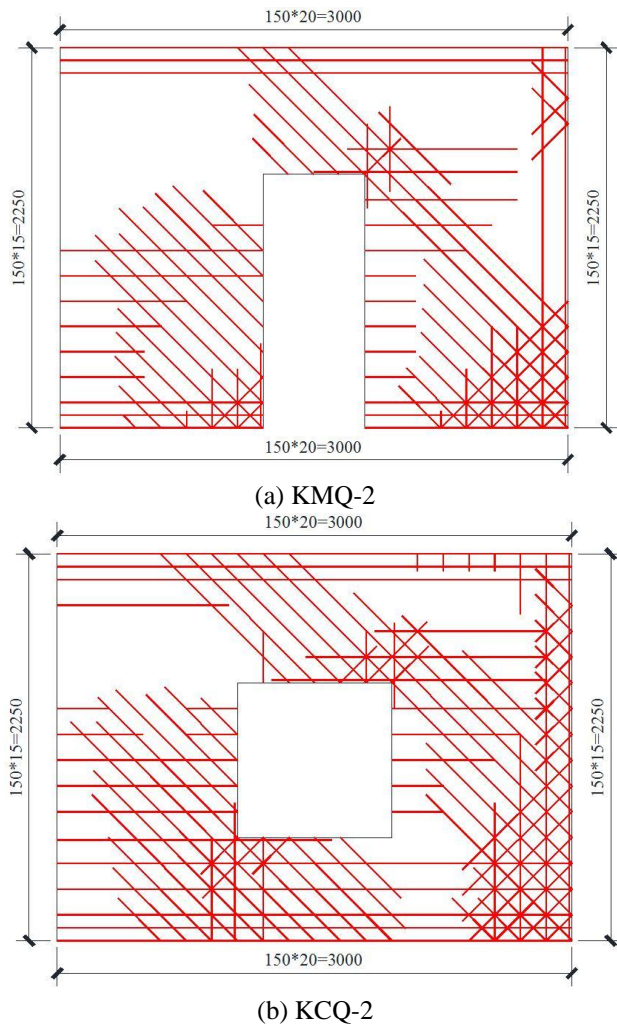


Fig. 6 Reinforcement layout of specimens designed using separated-elements model GESO method (Note: dimensions in mm; 1 in. = 25.4 mm; the design  $f_{y,k}$  of the reinforcements is 300 N/mm<sup>2</sup>, with a diameter of 6 mm; 1 ksi = 6.895 N/mm<sup>2</sup>)

Table 1 Steel usage

Type	Specimen	Main reinforcement (kg)	Wire mesh (kg)	Total (kg)	$m_1-m_2$ (kg)	$(m_1-m_2)/m_2$	$(M_1-M_2)/M_2$
A	KMQ-1	$m_1=36.36$	2.39	$M_1=38.75$	6.09	20.12%	18.65%
	KMQ-2	$m_2=30.27$		$M_2=32.66$			
B	KCQ-1	$m_1=45.81$	2.43	$M_1=48.24$	4.82	11.76%	11.10%
	KCQ-2	$m_2=40.99$		$M_2=43.42$			

\* $m_1$  = steel usage of the main reinforcement of a specimen designed using the elastic stress method;  $M_1$  = total steel usage of a specimen designed using the elastic stress method;  $m_2$  = steel usage for the main reinforcement of a specimen designed using the separated-elements model GESO method;  $M_2$  = total steel usage a specimen designed using the separated-elements model GESO method; 1 lb = 0.454 kg

layers). It should also be noted that some steel bars were slightly longer than those from topological results for ensuring the connections between the top beams and ground

Table 2 Properties of concrete

Type	Specimen	$f_{cu}$ (N/mm <sup>2</sup> )	$f_c$ (N/mm <sup>2</sup> )
A	KMQ-1	39.78	26.61
	KMQ-2		
B	KCQ-1	39.01	26.09
	KCQ-2		

\*1 ksi = 6.895 N/mm<sup>2</sup>

Table 3 Properties of reinforcement

Type	Diameter (mm)	$f_{ym}$ (N/mm <sup>2</sup> )	$\epsilon_{ym}$ (10 <sup>-6</sup> )	$f_{um}$ (N/mm <sup>2</sup> )
Chinese HPB300	6	436.20	1917	560.88
	8	387.94	1769	464.70
	10	424.41	1992	513.86
	12	415.57	1944	514.53
	14	374.61	1702	489.54
	16	318.31	1446	453.55

\*1 in. = 25.4 mm; 1 ksi = 6.895 N/mm<sup>2</sup>

beams and between the top beams and wall bodies; and a few slightly intermittent steel bars are merged for simplifying the fabrication.

### 3.5 Comparison of steel usage

The steel usage for the specimen is listed in Table 1. Table 1 indicates that a larger amount of reinforcement was needed for the specimens using the elastic stress method compared to that using the separated-elements model GESO method. In other words, nearly 10-20% of reinforcement could be saved if the separated-elements model GESO is utilized to design the specimens in this study.

### 3.6 Material properties

The same concrete mix was utilized for fabricating the four specimens. Twelve cubes with dimensions of 150 mm×150 mm×150 mm (5.9 in.×5.9 in.×5.9 in.) were cast and cured under a standard maintain condition as described in the Chinese code (GB 50010-2010 2010) (maintained at temperature of 20±3°C and humidity of greater than 90% for 28 days). During testing, each cube was placed on the bearing plate with no lubricating oil and its centerline was aligned with that of the bearing plate. Then, the test machine operated to lower down the upper plate (also with no lubricating oil) until the upper plate was in contact with the specimen. The loading rate was maintained in the range of about 0.5-0.8 N/mm<sup>2</sup> (0.0725-0.116 ksi) per second. The average cubic compressive strength value  $f_{cu}$  was obtained through standard cube testing. Based on the conversion approach given in the Chinese code (GB 50010-2010 2010), the axial compressive strength ( $f_c$ ) per the US code (ACI 318-14 2014) was obtained. The measured concrete material properties are shown in Table 2. Three bars were tested for each type of reinforcement and the average yield strength value  $f_{ym}$  and average ultimate tensile strength  $f_{um}$

were be obtained from tensile test results. The elastic modulus ( $E_0$ ) of the steel was  $2.1 \times 10^5$  N/mm<sup>2</sup> ( $3.05 \times 10^4$  ksi) according to Chinese code (GB 50010-2010 2010). The measured properties of reinforcement are shown in Table 3.

### 3.7 Loading plan

The specimen tests were conducted in the structure laboratory at Hunan University, Changsha, China. The horizontal loading device was a 1000 kN (224.8 kips) servo-controlled loading system. The vertical loading devices were three 1000 kN (224.8 kips) hydraulic jacks. The vertical loads were transformed into a uniform load by a spreader girder, ten roller supports, and a steel plate at the top of the top beam shown in Fig. 7(a). The ground beam was post-tensioned on the ground of the laboratory using anchors and thus there are restraints at its bottom surface due to the prestress and friction. The ground beam was also laterally supported at one end opposite to the horizontal loading. The lateral support relied on the gantry supporting the two sides of a specimen in order to avoid lateral buckling. The detailed test setup is shown in Fig. 7.

For each testing, a constant vertical load of around 866 kN (194.7 kips) was applied initially, consisting of three loads of 280 kN (62.9 kips) from three hydraulic jacks and self-weights of the jacks, force sensor, distributive girder, roller supports, steel plate, and top beam. Namely, the actual axial load ratios of Types A and B specimens were 0.090 and 0.092, respectively, based on the measured properties of the concrete. Next, a horizontal load was applied. A small load was preliminarily applied, reaching 100 kN (22.5 kips) (i.e., 50% of the estimated crack load) in two load steps. Before concrete cracking, the load increased by an increment of 40 kN (9.0 kips) in several steps, but the incremental load was changed to 20 kN (4.5 kips) when the load approached the estimated cracking load. After concrete cracking, the incremental load was set to 40 kN (9.0 kips) again. However, when the load was close to the design load, the incremental load was adjusted to 20 kN (4.5 kips). Before failure of the specimen, its displacement increased significantly while the load was slightly changed. Thus, the displacement was utilized to control the load until failure of the specimen. All tests would be terminated when the horizontal load values recorded by servo-controlled loading system dropped sharply. According to the data recorded during the test shown in the later sections, the main diagonal crack of every wall had reached a large width and there are some parts where concrete had been crushed at that time. It should be noted that, during the testing, the loads of the hydraulic jacks were slightly changed due to the movement of wall bodies which led to additional bending moment at the top of the walls. To ensure a constant axial load ratio, each hydraulic jack was adjusted at each load step to maintain a constant vertical load.

### 3.8 Instrumentation

During the tests, strain, loads, and displacement were measured and cracks were mapped. The vertical loads were recorded by load cells at the top of hydraulic jacks and the horizontal thrust was measured by a load cell attached at the

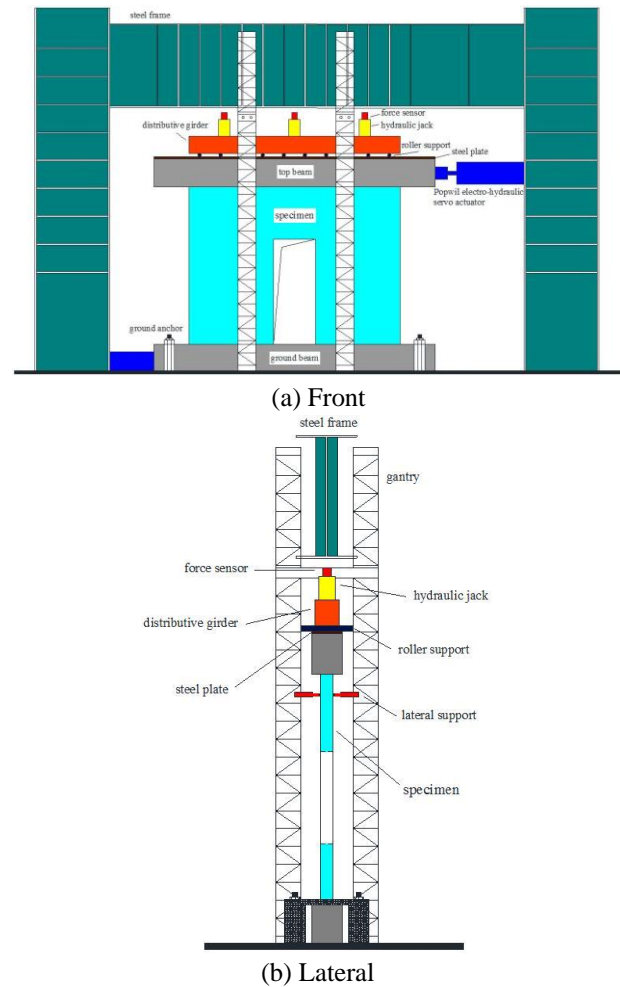


Fig. 7 Loading device

electro-hydraulic servo actuator. The displacement was collected by linear displacement sensors on the specimens. Strain gauges were also installed on the reinforcement and surface of the specimens.

The locations of displacement sensors are shown in Fig. 8. The two specimens of the same type have identical displacement measurement. The horizontal displacement at the top and middle areas was collected step by step. Besides, the slip at the bottom area, the rotation of each specimen, the horizontal displacements of the top beam and ground beam were also collected.

Type A specimens were taken as an example to illustrate the strain measurement locations as shown in Fig. 9. The reinforcement strain gauges were mainly mounted far away from the anchor ends to observe the stress development and yield of the reinforcement. The concrete strain gauges were installed on the compression region of the wall. A few gauges were installed at the tension side and middle of the wall in order to validate the use of the plane section assumption to designing shear walls. Additionally, the concrete strain at the tension region of the wall can reveal the potential crack formation.

## 4. Results and discussions

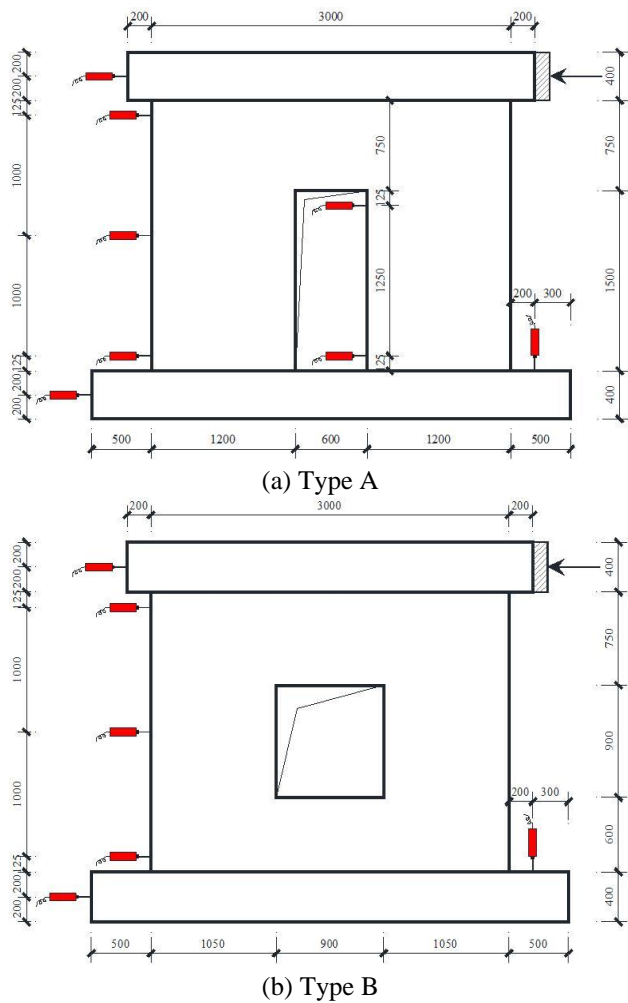
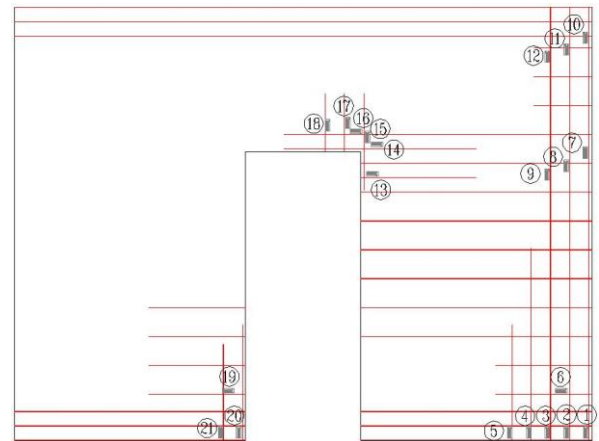


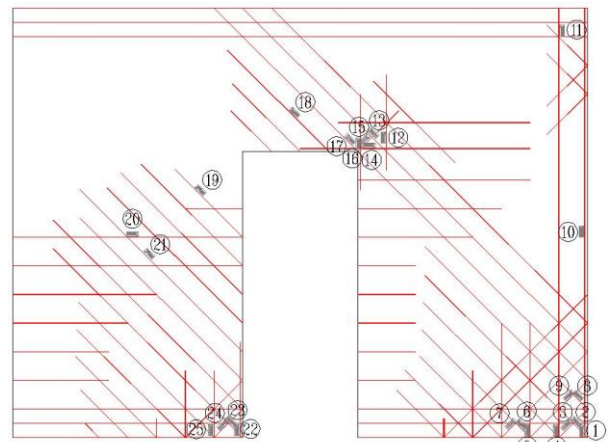
Fig. 8 Displacement sensor arrangement (Note: dimensions in mm; 1 in. = 25.4 mm.)

#### 4.1 The loads

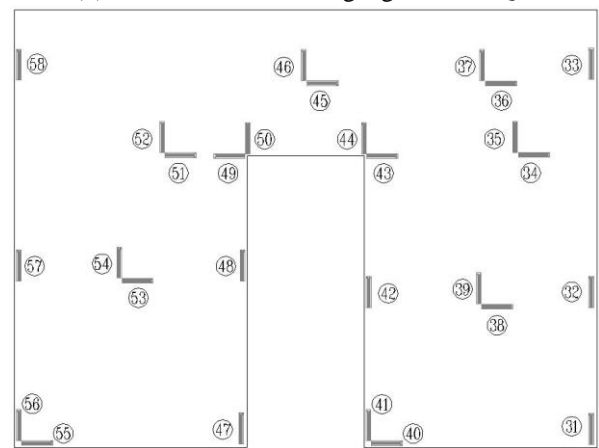
The crack load ( $F_{cr}$ ), yield load ( $F_y$ ), ultimate load ( $F_u$ ) of each specimen are shown in Table 4. No significant difference was found between the crack loads or ultimate loads of the two shear walls of the same type designed using the two methods respectively. The failure modes were also similar including the development of the diagonal crack and the concrete crush at the corner of the wall which led to failure (discussed in detail later). Likewise, the corresponding ratio of the ultimate load to the cracking load ( $F_u/F_{cr}$ ) was almost the same. However, the yielding loads of the shear walls designed using the two methods were significantly different. The shear walls designed by the separated-elements model GESO method had a larger yield ratios ( $F_u/F_y$ , the ratio of the ultimate load to the yield load), i.e., around 1.2-1.4. This indicates that the failure occurred obviously later than some reinforcements began to yield. The reinforcement could be used more effectively especially after the stress redistribution. On the other hand, the yield ratios of the shear walls designed using the elastic stress method were close to 1.0, which indicated that the shear walls were damaged immediately following the yield of the reinforcement.



(a) Reinforcement strain gauges of KMQ-1



(b) Reinforcement strain gauges of KMQ-2



(c) Concrete strain gauges of specimens KMQ-1 and KMQ-2

Fig. 9 Strain gauges arrangement of specimens KMQ-1 and KMQ-2

#### 4.2 Ultimate displacement and ductility

During each test, no significant slip was found at the interfaces between the top beam and the specimen and between the ground beam and the specimen. All supports and gantry worked well, and the out-of-plane movement of the wall body was negligible. Due to the limited stiffness of ground anchors, the rotation of the wall body could not be

Table 4 Measured loads

Type	Specimen	$F_{cr}$ (kN)	$F_y$ (kN)	$F_u$ (kN)	$F_u/F_{cr}$	$F_u/F_y$
A	KMQ-1	287	749	818	2.850	1.092
	KMQ-2	276	664	820	2.971	1.235
B	KCQ-1	187	784	799	4.273	1.019
	KCQ-2	173	565	793	4.584	1.404

1 kip = 4.448 kN

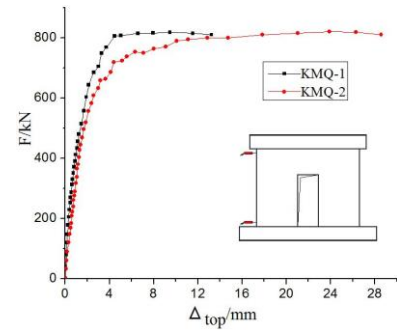
Table 5 Measured displacements

Type	Specimen	$\Delta_{cr}$	$\Delta_y$	$\Delta_0$	$\Delta_u$	$\Delta_u/\Delta_y$	$\Delta_u/H$
A	KMQ-1	0.544	3.289	9.482	13.235	4.024	0.00662 (1/151)
	KMQ-2	0.826	3.632	23.926	28.582	7.869	0.01429 (1/70)
B	KCQ-1	0.804	8.647	10.644	14.821	1.714	0.00741 (1/135)
	KCQ-2	0.832	4.631	15.964	25.587	5.525	0.01279 (1/78)

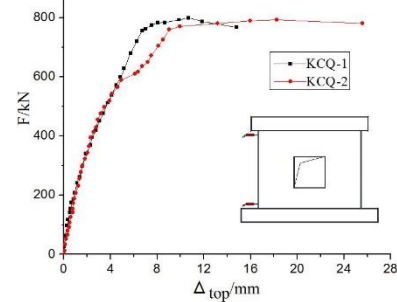
$H$  was the height difference between two linear displacement sensors at the top and bottom of the wall; displacements in m; 1 in. = 25.4 mm

ignored, but the influences were eliminated through deducting the errors caused by specimen rotation and can be converted by the rotation of ground beam which had recorded in the test with the help of a linear displacement sensors vertically set at the right end of the ground beam. The displacements ( $\Delta_{cr}$ ,  $\Delta_y$ ,  $\Delta_0$  correspond to  $F_{cr}$ ,  $F_y$ , and  $F_u$ , respectively;  $\Delta_u$  was the ultimate elastic-plastic displacement) and some parameters related to the ductility performance are listed in Table 5. The load-deformation curves are shown in Fig. 10. In Fig. 10,  $\Delta_{top}$  is the reading difference between two linear displacement sensors (shown in Fig. 8) at the top and the bottom of the walls deducting the effect of the rotation of the wall body.  $\Delta_{mid}$  is the reading difference between the two linear displacement sensors (shown in Fig. 8) at the middle depth and bottom of the walls deducting the effect of the rotation of the wall body.  $\Delta_{r-limb}$  is the reading difference between the two linear displacement sensors (shown in Fig. 8(a)) at the right wall limb of each Type A specimen deducting the effect of the rotation of the wall body. All displacements were measured relative to the initial state after applying the vertical loading.

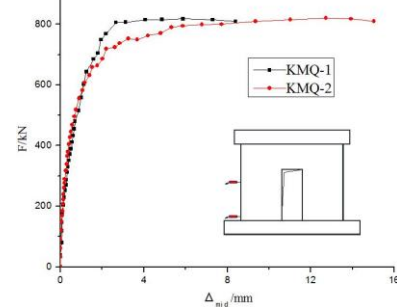
In Fig. 10, the loading-displacement curves of the shear walls designed using two methods overlap at the beginning. This is due to the fact that the stiffness of the structures was mostly dependent on the concrete before cracking while the specimens of the same type had same concrete properties and specimen dimensions. It can be concluded from Fig. 10 that the shear walls designed by the separated-elements model GESO method had better ductility considering longer platforms and greater ultimate elastic-plastic displacements. Especially, the ultimate elastic-plastic displacements were nearly twice as those of the specimens designed by the elastic stress method. Therefore, as listed in Table 5, the plastic angular displacement ( $\Delta_u/H$ ) and ductility coefficient ( $\Delta_u/\Delta_y$ ) of the shear walls designed by the separated-



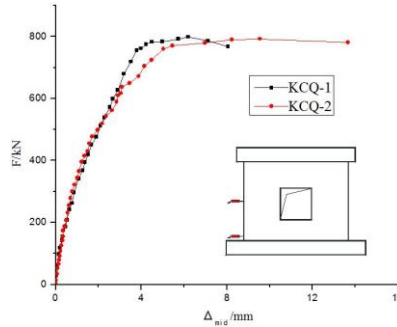
(a) The top of Type A specimens



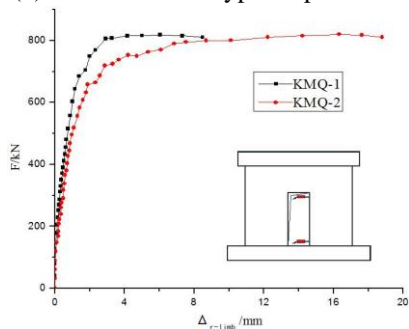
(b) The top of Type B specimens



(c) The middle of Type A specimens



(d) The middle of Type B specimens



(e) The right limbs of Type A specimens

Fig. 10 Loading-displacement curves (Note: 1 in. = 25.4 mm; 1 kip = 4.448 kN.)

Table 6 Relative stiffness

Type	Specimen	$k_0$	$k_{cr}$	$k_y$
A	KMQ-1	1.000	0.528	0.146
	KMQ-2	1.000	0.522	0.252
B	KCQ-1	1.000	0.662	0.241
	KCQ-2	1.000	0.704	0.413

elements model GESO method were much greater than that designed using the elastic stress method. Note that the measured results of the plastic angular displacement demonstrated the ultimate elastic-plastic deformability and the measured results of the ductility coefficient indicated the deformability of the walls from yield to failure. The two parameters are the important parameters for measuring the ductility of shear walls, suggesting the advantages of the separated-elements model GESO method in terms of ductility. It is also worth noting that the shear walls were initially in bending, behaved as a frame with the accumulation of damage, and finally showed shear failure characteristics.

4.3 Stiffness degradation

The relative cracking stiffness ( $k_{cr}$ ) and relative yielding stiffness ( $k_y$ ) are defined as follows

$$k_{cr} = K_{cr}/K_0 \tag{1}$$

$$k_y = K_y/K_0 \tag{2}$$

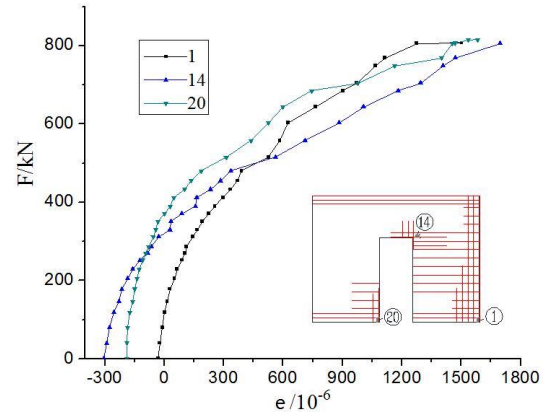
$K_0$  is initial elastic stiffness;  $K_{cr}$  is secant stiffness corresponding to cracking load; and  $K_y$  is secant stiffness corresponding to yielding load. The initial relative stiffness  $k_0 = 1.000$ . All relative rigidities are shown in Table 6.

It can be found from Table 6 that the stiffness degradation before cracking was dependent on the tensile strength of concrete and the dimensions of specimens. And the same type shear walls had almost the same stiffness degradation. Nevertheless, the shear walls designed using the separated-elements model GESO method had a lower rate of stiffness degradation after cracking, because their reinforcement layouts were more effective at constraining concrete cracks.

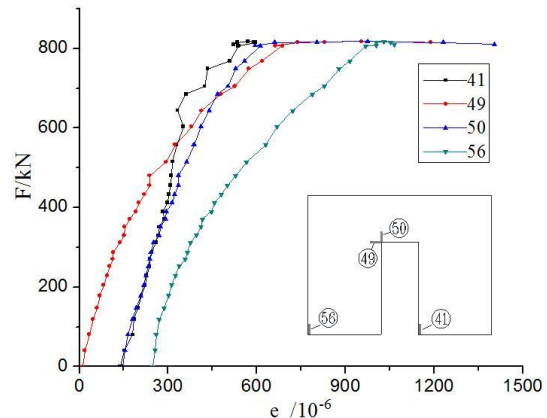
4.4 The strains

Due to similarities, Type A specimens are used to discuss the strain development and the effectiveness of the main reinforcement in the specimens. The load-strain curves for these specimens are shown in Fig. 11.

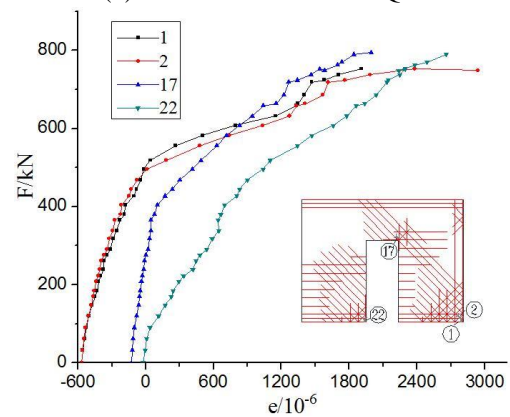
Based on the yield strain of the steel ( $\epsilon_{ym}$ ) from the material tests, the reinforcement of the specimens that yielded were identified. As shown in Fig. 11, only a few amount of reinforcement in specimen KMQ-1 yielded. Some horizontal reinforcement above the upper-right corner of the opening yielded at a load of 749 kN (168.4 kip); and some vertical reinforcement above the upper-right corner of the opening and at the bottom-right corner of the wall body yielded at the load of between 806 kN-815 kN (181.2 kip-



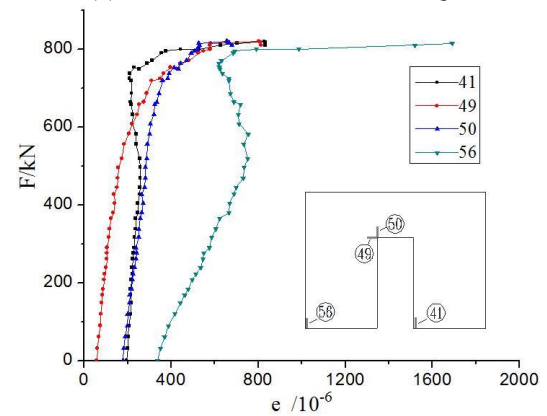
(a) Reinforcement strain of KMQ-1



(b) Concrete strain of KMQ-1



(c) Reinforcement strain of KMQ-2



(d) Concrete strain of KMQ-2

Fig. 11 Load-strain curves of Type A specimens (Note: 1 kip = 4.448 kN.)

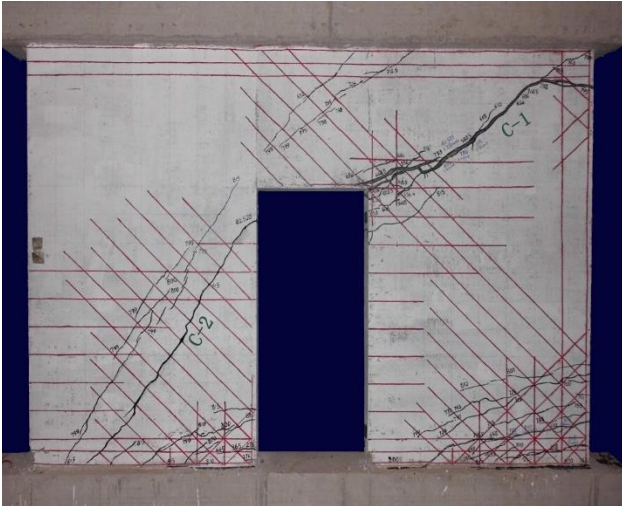


Fig. 12 Crack maps and failure modes of specimen KMQ-1 (Note: displacements and cracks widths in mm; 1 in. = 25.4 mm; loads in N/mm<sup>2</sup>; 1 ksi = 6.895 N/mm<sup>2</sup>)

183.2 kip). Most of the reinforcements in specimen KMQ-1 did not yield at the ultimate state, indicating it has little ductility after reinforcements yielded. However, lots of reinforcement in specimen KMQ-2 yielded successively before failure, indicating a good structural ductility. Almost all the vertical and diagonal reinforcements at the bottom-right corner of the wall body yielded successively at the load of between 718.5 kN (161.5 kips) and 810 kN (182.1 kips). Most of the vertical and diagonal reinforcements above the upper-right corner of the opening and beside the bottom-left corner of the opening also yielded, and especially one of the vertical reinforcement yielded at the load of 664 kN (149.3 kips).

There was little difference between the concrete strains in two shear walls of the same type; although the specimen designed using separated-elements model GESO method had slightly smaller strains. Moreover, the design of shear walls based on the plane-section assumption is unreasonable according to the concrete strain results at cross-sections of the shear walls.

In sum, the separated-elements model GESO method can be used to improve the ductility of shear walls, because the reinforcements can be more efficiently and effectively utilized such that most of reinforcements could yield before specimen failure. And the specimens designed using the separated-elements model GESO method had a ductile behavior similar to that of RC beams with a bending failure.

#### 4.5 Crack distribution and failure modes

The crack development, distribution and ultimate failure modes of the specimens are shown in Figs. 12-15. All cracks are painted on the wall bodies step-by-step according to the increasing loads and the crack width is also constantly updated to maximum measured value in real time. In Figs. 12-15, the red lines represent the reinforcements; the blue numbers represent the crack width; the black numbers with no decimal or one decimal near the cracks were the corresponding loads, and the ones with

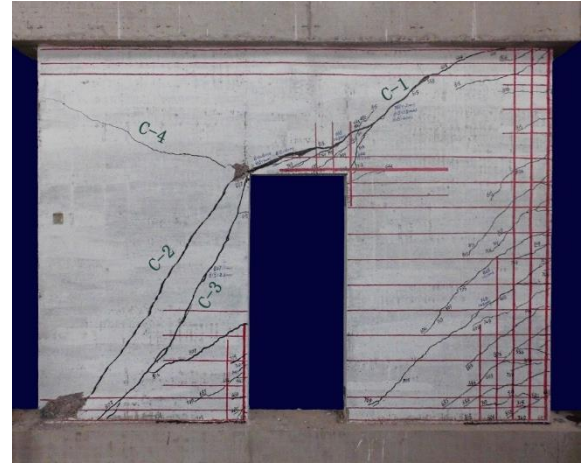


Fig. 13 Crack maps and failure modes of specimen KMQ-2 (Note: displacements and cracks widths in mm; 1 in. = 25.4 mm; loads in N/mm<sup>2</sup>; 1 ksi = 6.895 N/mm<sup>2</sup>)

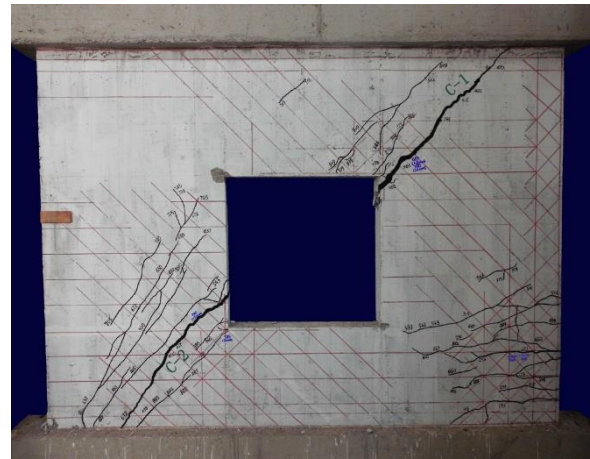


Fig. 14 Crack maps and failure modes of specimen KCQ-1 (Note: displacements and cracks widths in mm; 1 in. = 25.4 mm; loads in N/mm<sup>2</sup>; 1 ksi = 6.895 N/mm<sup>2</sup>)

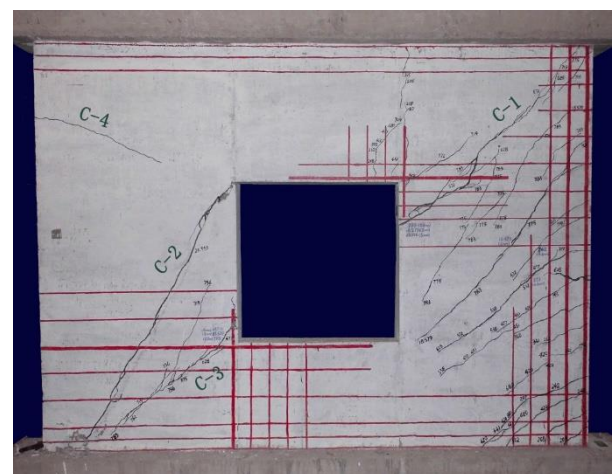


Fig. 15 Crack maps and failure modes of specimen KCQ-2 (Note: displacements and cracks widths in mm; 1 in. = 25.4 mm; loads in N/mm<sup>2</sup>; 1 ksi = 6.895 N/mm<sup>2</sup>)

three decimals were the corresponding displacement after reaching the maximum load.

The failure modes of the four specimens were similar: a diagonal crack from the loading point at the upper-right corner to the main compression area at the bottom-left corner of the wall body; the bottom-left corners of specimens KCQ-1 and KCQ-2 and the bottom-left corners of two wall limbs of specimens KMQ-1 and KMQ-2 crushed at failure.

However, there were some differences of crack development and failure modes between the shear walls of the same type designed using two methods:

1) Diagonal crack C-2 led to failure. Although the diagonal crack C-3 developed earlier, at failure the crack C-2 occurred suddenly with widths of exceeding 2 mm (0.079 in.) at their upper-left while the crack width of C-3 was still small and crack C-4 appeared at the upper-left of the wall body. The diagonal crack C-2 of specimens KCQ-2 and KMQ-2 appeared at the same place where crack C-3 was located at specimens KCQ-1 and KMQ-1. Diagonal crack C-2 developed moderately and led to failure finally.

2) The development of main cracks. In specimen KMQ-1, the maximum width of the main diagonal cracks C-1 and C-2 were nearly 10 mm (0.394 in.) at the final, and the width of the diagonal crack C-3 was 2.2 mm (0.087 in.). In specimen KCQ-1, the maximum widths of diagonal cracks C-1, C-2 and C-3 were all around 5 mm (0.197 in.) at failure. In specimen KMQ-2, the maximum width of main diagonal crack C-1 was 25 mm (0.984 in.), while in specimen KCQ-2, the maximum widths of main diagonal cracks C-1, C-2 were 24 mm (0.945 in.) and 15 mm (0.591 in.), respectively. Thus, the shear walls designed using separated-elements model GESO method had a better ability of accommodating concrete cracking.

3) Crack types. Lots of bending cracks at the bottom-right of specimens KMQ-2 and KCQ-2 developed extensively. Especially in KMQ-2, the maximum width of the bending cracks was 4 mm (0.157 in.). Few bending cracks existed in specimens KMQ-1 and KCQ-1, i.e., only two or three formed upward and become diagonal cracks.

4) The location comparison between reinforcements and cracks. Almost all the cracks in specimens KMQ-2 and KCQ-2 were perpendicular to some designed reinforcements. Reinforcements were more intensive at the locations where more cracks formed, and no crack existed at the locations without reinforcements. These phenomena were all consistent with the designs. In specimens KMQ-1 and KCQ-1, the cracks were also perpendicular to some designed reinforcements in the beginning, but they deviated along with the increase of the load due to the restraint from massive reinforcements. Finally, some cracks, which occurred at the locations without reinforcements, were parallel to the reinforcements or developed forward across the main reinforcements. These cracks exceeded the limits given by designs.

## 5. Conclusions

Shear walls are a typical member under a complex stress state and have complicated mechanical properties and failure modes. The separated-elements model GESO

method is a combination of an elastic-plastic stress method and optimization method for designing such members. It is quite different from the elastic stress method, but lacks validation against test results. In this research, the adequacy of the separated-elements model GESO method was validated against experimental data and compared with the traditional elastic stress method. Two types of RC shear wall specimens, which had the location of an opening in the middle bottom and the center region, respectively, were designed, fabricated, instrumented, and tested. For each type, two specimens were designed using the separated-elements model GESO method and elastic stress method, respectively. All specimens were subjected to a constant vertical load and an incremental lateral load until failure. For each wall type, the test results from the two specimens designed using the two methods respectively were compared. Specific conclusions were drawn as follows:

- The crack and ultimate loads of the specimens designed using separated-elements model GESO method and elastic stress method had no significant difference. However, the specimens designed using the separated-elements model GESO method had a bending type deformation compared to the shearing type deformation of the specimens designed using the elastic stress method as the damage accumulated.

- The specimens designed using separated-elements model GESO method had a more obvious bending behavior, more extensive crack development, larger plastic angular displacements, higher ductility coefficient, and moderate stiffness degradation. Accordingly, the separated-elements model GESO method can be utilized to improve the ductility of shear walls.

- The separated-elements model GESO method could be used to intuitively obtain the reinforcement layout of shear walls under a complex stress state, including the locations, lengths, and quantity of steel bars. The resulting reinforcement layout was more accurate at capturing cracks. The reinforcements were utilized more effectively, reducing the need of steel usage.

## Acknowledgments

The work described in this paper was fully funded by the National Science Foundation of China (Project No: 51508182 and 51338004).

## References

- ACI 318 (2014), *Building Code Requirements for Structural Concrete and Commentary*, American Concrete Institute, Michigan, U.S.A.
- ASCE/SEI 41-06 (2007), *Seismic Rehabilitation of Existing Buildings*, American Society of Civil Engineers, 180-193.
- Christidis, K.I. and Trezos, K.G. (2017), "Experimental investigation of existing non-conforming RC shear walls", *Eng. Struct.*, **140**, 26-38.
- Fernandes, W.S., Greco, M. and Almeida, V.S. (2017), "Application of the smooth evolutionary structural optimization method combined with a multi-criteria decision procedure", *Eng. Struct.*, **143**, 40-51.

- GB 50010 (2010), *Code for Design of Concrete Structures*, Ministry of Housing and Urban-Rural Development of the People's Republic of China, Beijing, China.
- Galano, L. and Vignoli, A. (2000), "Seismic behavior of short coupling beams with different reinforcement layouts", *ACI Struct. J.*, **97**(6), 876-885.
- Gulec, C.K., Whittaker, A.S. and Stojadinovic, B. (2008), "Shear strength of squat rectangular reinforced concrete walls", *ACI Struct. J.*, **105**(4), 488-497.
- Javidsharifi, B. (2017), "Distribution of strength and stiffness in asymmetric wall type system buildings considering foundation flexibility", *Struct. Eng. Mech.*, **63**(3), 281-292.
- JGJ 3 (2010), *Technical Specification for Concrete Structures of Tall Building*, Ministry of Housing and Urban-Rural Development of the People's Republic of China, Beijing, China.
- Lao, X.C. and Han, X.L. (2011), "Performance index limits of medium-height RC shear wall components", *Adv. Mater. Res.*, 163-167, 1134-1138.
- Liang, X.W., Kou, J.L. and Deng, M.K. (2011), "Experimental investigation on seismic behaviors of high-performance concrete shear walls of rectangular section", *Adv. Mater. Res.*, 255-260, 2439-2443.
- Liu, X. and Yi, W.J. (2010), "Michell-like 2D layouts generated by genetic ESO", *Struct. Multidiscipl. Optim.*, **42**, 111-123.
- Liu, X., Yi, W.J., Li, Q.S. and Shen, P.S. (2008), "Genetic evolutionary structural optimization", *J. Constr. Steel Res.*, **64**, 305-311.
- Pavel, F. and Pricopie, A. (2015), "Prediction of engineering demand parameters for RC wall structures", *Struct. Eng. Mech.*, **54**(4), 741-754.
- Querin, O.M. (1997), "Evolutionary structural optimisation: Stress based formulation and implementation", Ph.D. Dissertation, University of Sydney, Sydney, Australia.
- Querin, O.M., Steven, G.P. and Xie, Y.M. (1998), "Evolutionary structural optimisation (ESO) using a bidirectional algorithm", *Eng. Comput.*, **15**(8), 1031-1048.
- Querin, O.M., Young, V., Steven, G.P. and Xie, Y.M. (2000), "Computational efficiency and validation of bi-directional evolutionary structural optimisation", *Comput. Meth. Appl. Mech. Eng.*, **189**(2), 559-573.
- Quiroz, L.G., Maruyama, Y. and Zavala, C. (2013), "Cyclic behavior of thin RC peruvian shear walls: Full-scale experimental investigation and numerical simulation", *Eng. Struct.*, **52**(9), 153-167.
- Salonikios, T.N. (2002), "Shear strength and deformation patterns of R/C walls with aspect ratio 1.0 and 1.5 designed to Eurocode 8 (EC8)", *Eng. Struct.*, **24**(1), 39-49.
- Salonikios, T.N., Kappos, A.J., Tegos, I.A. and Penelis, G.G. (1999), "Cyclic load behavior of low-slenderness reinforced concrete walls: Design basis and test results", *ACI Struct. J.*, **96**(4), 649-660.
- Tang, Y., Kurtz, A. and Zhao, Y.F. (2015), "Bidirectional evolutionary structural optimization (BESO) based design method for lattice structure to be fabricated by additive manufacturing", *Comput.-Aid. Des.*, **69**(C), 91-101.
- Tomazevic, M., Lutman, M. and Petkovic, L. (1996), "Seismic behavior of masonry walls: Experimental simulation", *J. Struct. Eng.*, **122**(9), 1040-1047.
- Xie, Y.M. and Steven, G.P. (1993), "A simple evolutionary procedure for structural optimization", *Comput. Struct.*, **49**(5), 885-896.
- Yang, X.Y., Xie, Y.M., Steven, G.P. and Querin, O.M. (1999), "Bidirectional evolutionary method for stiffness optimization", *AIAA J.*, **37**(11), 1483-1488.
- Young, V., Querin, O.M., Steven, G.P. and Xie, Y.M. (1999), "3D and multiple load case bi-directional evolutionary structural optimization (BESO)", *Struct. Optim.*, **18**(2-3), 183-192.
- Zhang, H.Z., Liu, X. and Yi, W.J. (2014), "Reinforcement layout optimisation of RC D-regions", *Adv. Struct. Eng.*, **17**(7), 979-992.
- Zhang, W.X., Huang, X. and Liu, X. (2017), "Reinforcement layout optimization design using the genetic adding evolutionary structural optimization", *J. Comput. Mech.*, **34**(3), 303-311.

CC